Mechanism and Machine Theory 61 (2013) 156–167

Contents lists available at SciVerse ScienceDirect

Mechanism and Machine Theory

journal homepage: www.elsevier.com/locate/mechmt

A theoretical study of weight-balanced mechanisms for design of spring assistive mobile arm support (MAS)

Po-Yang Lin [a], Win-Bin Shieh [b], Dar-Zen Chen [a,*]

[a] Dept. of Mechanical Engineering, National Taiwan University, Taipei 10617, Taiwan
[b] Dept. of Mechanical Engineering, Ming Chi University of Technology, New Taipei 24301, Taiwan

ARTICLE INFO

Article history:
Received 3 April 2011
Received in revised form 10 August 2012
Accepted 12 November 2012

Keywords:
Mobile arm support
Gravity balance
Stiffness matrix
Upper limb exoskeleton

ABSTRACT

This paper studies the underlying theory of weight-balanced mechanism for the design of a class of spatial mobile arm support (MAS), a spring assistive MAS. Conventional designs of spring assistive MAS and their associated spring balancing techniques are analyzed based on the stiffness matrix analysis in order to highlight the structural novelty of the proposed MAS design concept. This MAS comprises two ideal zero-free-length springs directly installed to the arm mechanism without using any auxiliary link. Through the passive assistance provided by the springs, the MAS can facilitate the arm movement in space by the complete weight compensation of the upper limb at any possible posture. The design is believed to have benefited from its simple structure and the easiness of adjustment compared to other conventional designs. The conceptual design of the MAS is proposed and followed with a simulation model. The gravity balancing is verified with an example of a quasi-static motion. The results show that the MAS is capable of fully balancing the weights of user's upper limb and the device during the full range of motion.

1. Introduction

Mobile arm supports (MASs) are the mechanical devices that support the weight of the arm and so provide assistance to shoulder and elbow motions through a linkage of low friction joints [1]. MASs were originally designed to increase independence for feeding function, but they have subsequently enabled thousands of people with upper extremity impairments to achieve other functional activities, including grooming, hygiene, writing, telephoning, household tasks, and recreational and vocational activities [2]. Various types of MASs have been proposed over years, such as the foot-operated feeder by the Georgia Warm Springs Foundation back in 1936 [3], the Barker Feeder by E. H. Barker at about the same time, the Jaeco MAS around 1950s [4], and recently the WREX [5,6], the ARMON [7] and the Freebal [8].

Limitations of the traditional MAS design include its conspicuous appearance, problems of doorway clearance, and the complexity of fitting the device for individual users to engage in particular activities. Nowadays, several applicable MASs are preferably designed in form of passive exoskeleton devices, suggesting no actuators and sensors being used, these devices can be safer, less expensive and even lighter. The exoskeleton-type MAS design is structurally and kinematically aligned to the arm of the user, this facilitates in navigating the arm through doorways and narrow spaces, and also, the applied assistive forces can be transmitted more uniformly on the subject's arm.

Without actuators and sensors, gravity balancing techniques are required to passively counterbalance the gravitational forces of the arm and the MAS itself. Passive gravity balancing technique in mechanisms is able to achieve the complete gravity compensation at *any* configuration of the mechanism. A MAS with passive gravity balancing function can provide the exact amount of support at any possible posture of the arm without overstretching it. Passive gravity balancing technique encompasses

* Corresponding author. Tel.: +886 2 3366 2723; fax: +886 2 2363 1755.
E-mail address: dzchen@ntu.edu.tw (D.-Z. Chen).

0094-114X/$ – see front matter © 2012 Elsevier Ltd. All rights reserved.
http://dx.doi.org/10.1016/j.mechmachtheory.2012.11.003

a variety of methods, e.g. the counterweight methods [9,10], the cam linkage methods [11,12] and the spring balancing methods [13–19]. Among these, the spring balancing methods are particularly favorable for the MASs since spring elements can be generally benefited from the light weight, small additional inertia, easiness for adjustments and cheap cost.

Most conventional spring balancing techniques use auxiliary links or linkages added to the mechanism to provide suitable attachment points for the springs [15–19]. However, the auxiliary links increase the system inertia as well as its structural complexity. This paper discloses the underlying theory of some of the famous spring balancing techniques and presents a theoretical study for the design of a class of a spatial spring assistive MAS without using auxiliary links, which is believed to be a novel design concept, simple in structure, and easy to be adjusted for individuals of distinct arm length and weight.

The layout of this paper is as follows. Section 2 presents the principle of gravity balancing techniques with springs. A general gravity-spring system is described by a stiffness matrix proposed by Lin et al. [14]. In Section 3, two existing spring balancing techniques using the auxiliary link method, which are both applied to planar 2-DOF (degree of freedom) serial kinematic chains, are investigated. In Section 4, a planar 2-DOF spring balancing arm without using auxiliary links is proposed. In Section 5, the planar 2-DOF design is extended to a spatial 4-DOF MAS by two additional rotational DOFs on the shoulder to accommodate the spatial kinematics of the upper extremity. With only two embedded springs, the 4-DOF MAS is capable of achieving static balance in spatial motion. In Section 6, a methodology for tuning the level of gravity compensation is proposed. The MAS is modeled and simulated in ADAMS. The simulated results shown in Section 7 justify the gravity balancing capability of the design.

2. Principle of gravity balancing with springs

2.1. The stiffness block matrix representation

To generally describe the configuration of a planar n-link articulated mechanism, let $\mathbf{q}_i$ be a unit vector fixed on link i ($i=1, 2, \ldots, n$) of the mechanism where link 1 is ground. The n-dimensional vector space spanned by $\mathbf{q}_1, \mathbf{q}_2, \ldots, \mathbf{q}_n$ defines the configuration of the mechanism. In the system, assume that all springs are *zero-free-length springs* working within their linear ranges, and the spring forces and the gravitational forces are conservative forces and configuration dependent. Hence, any force vector $\mathbf{f}$, can be expressed in a linear combination of $\mathbf{q}_i$'s as

$$\mathbf{f} = \sum_i \mathbf{F}_i \mathbf{q}_i \tag{1}$$

where $\mathbf{F}_i$ is a 2×2 constant coefficient matrix of $\mathbf{q}_i$, representing the rotation and scaling of $\mathbf{q}_i$.

Denote $\mathbf{p}$ as the position vector from the origin of the global coordinate system to the point where the force $\mathbf{f}$ is applied. For example, if $\mathbf{f}$ is the gravitational force of a link and $\mathbf{p}$ is the position vector of the mass center of the link, $\mathbf{p}$ can be expressed as

$$\mathbf{p} = \sum_i \mathbf{P}_i \mathbf{q}_i \tag{2}$$

where $\mathbf{P}_i$ is a 2×2 constant coefficient matrix of $\mathbf{q}_i$, representing the rotation and scaling of $\mathbf{q}_i$.

Hence, the potential energy contributed by the forces and their associated positions can be obtained as

$$U = \int \mathbf{f}^{\mathrm{T}} d\mathbf{p} = \sum_{i,j} \mathbf{q}_i{}^{\mathrm{T}} \mathbf{K}_{ij} \mathbf{q}_j \tag{3}$$

where $\mathbf{K}_{ij}$ is a 2×2 constant matrix derived from Eqs. (1) and (2) as

$$\mathbf{K}_{ij} = \mathbf{F}_i{}^{\mathrm{T}} \mathbf{P}_j. \tag{4}$$

Component matrix $\mathbf{K}_{ij}$ is the potential energy due to a relative angular position $\theta_{ij} = \cos^{-1}(\mathbf{q}_i{}^{\mathrm{T}}\mathbf{q}_j)$ of links i and j, and is also referred to as the stiffness component matrix between links i and j [14]. Hence, matrix $\mathbf{K}_{ij}$ is in energy unit, e.g. N–m.

In the spring-gravity system, both the gravitational potential energy U_{G} and the elastic potential energy U_{E} can be expressed in the form of Eq. (3). The total potential energy of the system U_{T}, i.e. the sum of U_{G} and U_{E}, can be further written in a block matrix form as

$$U_{\mathrm{T}} = \frac{1}{2} \mathcal{Q}^T \mathcal{K} \mathcal{Q} \tag{5}$$

where $\mathcal{K}$ and $\mathcal{Q}$ are respectively $2n\times2n$ and $2n\times1$ matrices as

$$\mathcal{K} = \left[\mathbf{K}_{ij}\right] \tag{6}$$

$$\mathcal{Q} = [\mathbf{q}_i]. \tag{7}$$

$\mathcal{K}$ and $\mathcal{Q}$ are respectively referred to as the stiffness block matrix and the configuration block matrix [14]. Note that, although the configuration matrix varies as the configuration of a mechanism changes, the stiffness block matrix is constant for a prescribed mechanism. Consider a simplified case where $\mathbf{q}_i$'s are respectively parallel to the line connecting the joint centers on link i in an articulated kinematic chain, and the local position vectors of all points of application, i.e., the position vectors of the mass centers and the spring attachment points, are respectively parallel to the corresponding local unit vector $\mathbf{q}_i$. In this case, matrices $\mathbf{F}_i$ and $\mathbf{P}_i$ are both 2×2 scalar matrices, and $\mathbf{K}_{ij}=K_{ij}\mathbf{I}$ where $\mathbf{I}$ denotes the 2×2 identity matrix. Derived from Eq. (3), the virtual work done by all working forces acting on the mechanism during any virtual configuration change is

$$\delta U_{\mathrm{T}} = K_{ij}\delta\left(\mathbf{q}_i^{\mathrm{T}}\mathbf{q}_j\right). \tag{8}$$

Thus,

$$\delta U_{\mathrm{T}} = \sum_{i,j,k} K_{ij}\left[\mathbf{q}_i^{\mathrm{T}}\frac{\partial\mathbf{q}_j}{\partial\theta_k}+\frac{\partial\mathbf{q}_i^{\mathrm{T}}}{\partial\theta_k}\mathbf{q}_j\right]\delta\theta_k \tag{9}$$

where θ_k ($k=2, 3,\ldots, n$) is the joint angle of link k, and its associated coefficient is the static joint torque.

If $i=j=k$ in Eq. (9), vectors $\mathbf{q}_i$ and $(\partial\mathbf{q}_i/\partial\theta_i)$ are perpendicular, and thus $\mathbf{q}_i^{\mathrm{T}}(\partial\mathbf{q}_i/\partial\theta_i)$ is zero. According to the *principle of virtual work*, the necessary and sufficient condition for the equilibrium of a mechanism is zero virtual work done by all working forces acting on the mechanism during any virtual configuration change. Hence, in an equilibrium system, for any $i\neq j$ in Eq. (9), all K_{ij}'s must be zero. That is, the stiffness block matrix becomes a diagonal matrix with all off-diagonal component matrices $\mathbf{K}_{ij}$'s being zero matrices. The potential energy is constant and independent of the configuration change of the mechanism and can be expressed as

$$U_{\mathrm{T}} = \frac{1}{2}\mathrm{tr}(\mathcal{K}_G+\mathcal{K}_E). \tag{10}$$

where $\mathcal{K}_{\mathrm{G}}$ and $\mathcal{K}_{\mathrm{E}}$ are the respective stiffness block matrices due to the gravitational forces and the spring forces.

The mechanism satisfying Eq. (10) is gravity balanced, i.e., the mechanism is in static equilibrium state at any configuration.

2.2. The gravitational stiffness block matrix of a 2-DOF serial chain

Consider a model of the MAS attached to the arm constrained in a vertical plane as shown in Fig. 2 where J_1 and J_2 are the revolute joint centers on the shoulder and the elbow, respectively. L is the length of the upper arm. m_2 and m_3 are the masses on the upper arm and the forearm, respectively. The position vector $\mathbf{c}$ of the overall mass center of the upper arm and the forearm, from reference point J_1, can be derived using $(m_2+m_3)\mathbf{c}=m_2(s_2\mathbf{q}_2)+m_3(L\mathbf{q}_2+s_3\mathbf{q}_3)$ where $\mathbf{q}_2$ and $\mathbf{q}_3$ are the unit vectors of the upper arm and the forearm, respectively, as shown in Fig. 2. Thus,

$$\mathbf{c} = c_2\mathbf{q}_2 + c_3\mathbf{q}_3 \tag{12}$$

where

$$c_2 = (m_2s_2 + m_3L)/(m_2+m_3) \tag{13}$$

$$c_3 = m_3s_3/(m_2+m_3). \tag{14}$$

Fig. 1. Different types of the existing MAS devices: (a) The original Jaeco MAS for subjects with severe shoulder girdle weakness [4]; (b) The Jaeco multi-link MAS with elevation assist [4]; (c) The WREX [5].

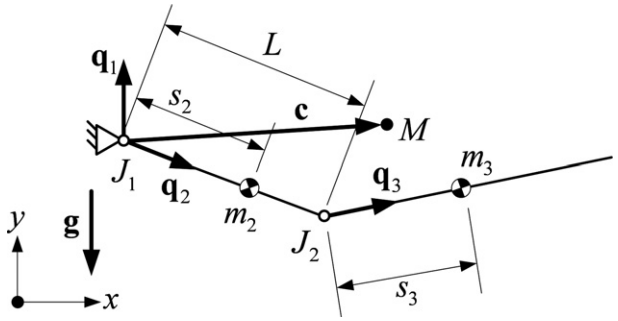

Fig. 2. The two-link model of upper limb.

The total gravitation potential energy of the system, according to Eq. (3), is

$$U_G = (\mu g \mathbf{q}_1)^{\mathrm{T}} \mathbf{c} = \mu g c_2 \mathbf{q}_1{}^{\mathrm{T}} \mathbf{q}_2 + \mu g c_3 \mathbf{q}_1{}^{\mathrm{T}} \mathbf{q}_3 \tag{15}$$

where $\mu = m_2 + m_3$, $-g\mathbf{q}_1$ is the gravitational acceleration vector $\mathbf{g}$, and $-\mu \mathbf{g}^{\mathrm{T}} \mathbf{q}_1$ is the gravitational force acting on the overall mass center of the system.

Since $\mathbf{q}^{\mathrm{T}}{}_i \mathbf{q}_j$ is a scalar, $\mathbf{q}^{\mathrm{T}}{}_i \mathbf{q}_j = (\mathbf{q}^{\mathrm{T}}{}_i \mathbf{q}_j)^{\mathrm{T}} = \mathbf{q}^{\mathrm{T}}{}_j \mathbf{q}_i$. Thus, the 6×6 stiffness block matrix due to gravity can be derived from Eq. (15) as a symmetric matrix,

$$\mathcal{K}_G = \begin{bmatrix} \mathbf{0} & \frac{1}{2}\mu g c_2 \mathbf{I} & \frac{1}{2}\mu g c_3 \mathbf{I} \\ & \mathbf{0} & \mathbf{0} \\ \text{sym} & & \mathbf{0} \end{bmatrix}. \tag{16}$$

where 'sym' represents the symmetric part of the stiffness block matrix.

3. Analysis of the existing planar 2-DOF spring balancing mechanisms with parallel auxiliary links

In this section, two existing spring balancing techniques are analyzed and compared based on the stiffness block matrix methodology.

3.1. The parallelogram linkage

Utilizing a single pendulum [16,17] and a four-bar parallelogram linkage [17,20] in the spring balancing mechanisms are well known techniques. The WREX and the Jaeco MAS both comprise a fundamental parallelogram linkage in the vertical plane for the gravity balance. A simplified illustration for such gravity balancing mechanisms is shown in Fig. 3, where k_1 and k_2 are the spring constants of the two 'ideal' zero-free-length extension springs. For an ideal zero-free-length spring, the spring force is proportional to the deformed magnitude of the spring. Through a cable–pulley system or alignment shafts [16,17,20,21], the spring length of a non-zero-free-length spring can be manipulated to match the desired spring force. Direct installation of a normal spring can also work equivalently as a zero-free-length spring if the normal spring is operated in a preload equal to its free length multiplied by the spring constant.

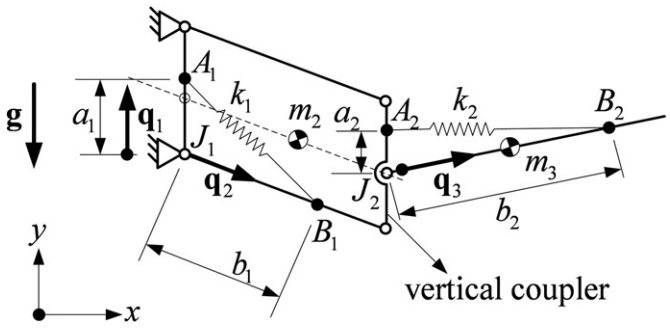

Fig. 3. The spring arrangement using the parallelogram linkage.

The elastic potential energy of spring k_1 can be written as

$$\begin{aligned} U_{E,1} &= \frac{1}{2}k_1(\mathbf{b_1}-\mathbf{a_1})^{\mathrm{T}}(\mathbf{b_1}-\mathbf{a_1}) \\ &= \frac{1}{2}k_1(b_1\mathbf{q}_2-a_1\mathbf{q}_1)^{\mathrm{T}}(b_1\mathbf{q}_2-a_1\mathbf{q}_1) \\ &= -k_1a_1b_1\mathbf{q}_1{}^{\mathrm{T}}\mathbf{q}_2+\frac{1}{2}k_1a_1{}^2\mathbf{q}_1{}^{\mathrm{T}}\mathbf{q}_1+\frac{1}{2}k_1b_1{}^2\mathbf{q}_2{}^{\mathrm{T}}\mathbf{q}_2 \end{aligned} \tag{17}$$

where $\mathbf{a}_1 = a_1\mathbf{q}_1$ and $\mathbf{b}_1 = b_1\mathbf{q}_2$ are the vectors pointing from point J_1 to the attachment points A_1 and B_1, respectively.

The stiffness block matrix induced by spring k_1 can be obtained as

$$\mathcal{K}_{E,1} = \begin{bmatrix} \frac{1}{2}k_1a_1{}^2\mathbf{I} & -\frac{1}{2}k_1a_1b_1\mathbf{I} & \mathbf{0} \\ & \frac{1}{2}k_1b_1{}^2\mathbf{I} & \mathbf{0} \\ \text{sym} & & \mathbf{0} \end{bmatrix}. \tag{18}$$

Due to the geometric constraint of the parallelogram, the coupler link of the parallelogram linkage remains vertical at any configuration. The spring-loaded forearm link mounted on the vertical coupler is thus considered similar to a ground-based, spring-loaded single pendulum. Although the attachment point A_2 is not fixed on ground, vector $\mathbf{a}_2$ pointing from point J_2 to point A_2 can be expressed as $a_2\mathbf{q}_1$. The elastic potential energy of spring k_2 can be written as

$$\begin{aligned} U_{E,2} &= \frac{1}{2}k_2(b_2\mathbf{q}_3-a_2\mathbf{q}_1)^{\mathrm{T}}(b_2\mathbf{q}_3-a_2\mathbf{q}_1) \\ &= -k_2a_2b_2\mathbf{q}_1{}^{\mathrm{T}}\mathbf{q}_3+\frac{1}{2}k_2a_2{}^2\mathbf{q}_1{}^{\mathrm{T}}\mathbf{q}_1+\frac{1}{2}k_2b_2{}^2\mathbf{q}_3{}^{\mathrm{T}}\mathbf{q}_3 \end{aligned} \tag{19}$$

where $b_2\mathbf{q}_3$ is the vector pointing from point J_2 to point B_2.

Hence, the stiffness block matrix is

$$\mathcal{K}_{E,2} = \begin{bmatrix} \frac{1}{2}k_2a_2{}^2\mathbf{I} & \mathbf{0} & -\frac{1}{2}k_2a_2b_2\mathbf{I} \\ & \mathbf{0} & \mathbf{0} \\ \text{sym} & & \frac{1}{2}k_2b_2{}^2\mathbf{I} \end{bmatrix}. \tag{20}$$

Having the off-diagonal component matrices $\mathbf{K}_{12}$, $\mathbf{K}_{13}$ and $\mathbf{K}_{23}$ of the summed stiffness block matrix of Eqs. (16), (18) and (20) as zero matrices yield the design equations of the gravity balanced linkage as shown in Fig. 3 as:

$$-k_1a_1b_1+\mu gc_2 = 0 \tag{21}$$

$$-k_2a_2b_2+\mu gc_3 = 0 \tag{22}$$

Eqs. (21) and (22) show the advantages of the parallelogram method, in which the two spring parameters can be selected or calibrated independently. The WREX and the Jaeco MAS use elastic bands instead of metal springs as shown in Fig. 1 which are even lighter and less apparent. By adding two revolute joints with vertical joint axes respectively on the vertical coupler and the base, the parallelogram can rotate about line J_1A_1, the forearm link can rotate about line J_2A_2, and the MAS can accommodate to the spatial motion of the arm without affecting its gravity balancing. As a result, the WREX has two DOFs on the shoulder and two DOFs on the elbow joints. In general, the glenohumeral joint and the elbow joint of a human upper extremity are generally treated as a 3-DOF spherical joint and a 1-DOF revolute joint, respectively, allowing the shoulder azimuth rotation, the shoulder elevation,

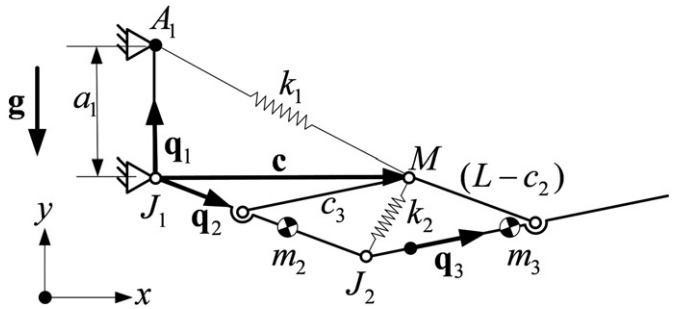

Fig. 4. The spring arrangement of the pantograph design.

the shoulder roll, and the elbow flexion–extension [22–24]. Although the WREX possesses the same DOF as the human upper extremity, shoulder roll motion is infeasible, because the parallelogram linkage must be 'rigidly' attached to the upper arm and be placed in a vertical-plane. Therefore, most MASs comprising the parallelogram linkages provide the assistive force with its fixer only on the subject's forearm as shown in Fig. 1(b) and (c). The balancing accuracy of most parallelogram MAS designs relies on the correct setup of $\mathbf{a}_1$ and $\mathbf{a}_2$ which is also commonly perceived as a disadvantage for such parallelogram linkage MAS.

3.2. The pantograph linkage

Agrawal et al. [18] proposed an alternative arrangement of auxiliary links and springs for spring balanced mechanisms [17]. The schematic of such a balancing mechanism is shown in Fig. 4, where the auxiliary links are used to locate the mass center M of the system and the mechanism is topologically similar to a pantograph linkage. The link lengths of the auxiliary links are evaluated based on the parameters c_3 and $(L-c_2)$ given in Eq. (12). Since spring k_1 connects the mass center M of the system and point A_1 on ground, the elastic potential energy of spring k_1 can be derived as

$$U_{E,1} = \frac{1}{2}k_1(\mathbf{c}-a_1\mathbf{q}_1)^{\mathrm{T}}(\mathbf{c}-a_1\mathbf{q}_1). \tag{23}$$

Substituting Eq. (12) into Eq. (23) yields

$$U_{E,1} = -k_1a_1c_2\mathbf{q}_1{}^{\mathrm{T}}\mathbf{q}_2 - k_1a_1c_3\mathbf{q}_1{}^{\mathrm{T}}\mathbf{q}_3 + k_1c_2c_3\mathbf{q}_2{}^{\mathrm{T}}\mathbf{q}_3 + \frac{1}{2}k_1a_1{}^2\mathbf{q}_1{}^{\mathrm{T}}\mathbf{q}_1 + \frac{1}{2}k_1c_2{}^2\mathbf{q}_2{}^{\mathrm{T}}\mathbf{q}_2 + \frac{1}{2}k_1c_3{}^2\mathbf{q}_3{}^{\mathrm{T}}\mathbf{q}_3. \tag{24}$$

The quadratic form of Eq. (24) yields the stiffness block matrix as

$$\mathbf{K}_{E,1} = \begin{bmatrix} \frac{1}{2}k_1a_1{}^2\mathbf{I} & -\frac{1}{2}k_1a_1c_2\mathbf{I} & -\frac{1}{2}k_1a_1c_3\mathbf{I} \\ & \frac{1}{2}k_1c_2{}^2\mathbf{I} & \frac{1}{2}k_1c_2c_3\mathbf{I} \\ \text{sym} & & \frac{1}{2}k_1c_3{}^2\mathbf{I} \end{bmatrix}. \tag{25}$$

Spring k_2 is fitted diagonally in the parallelogram as shown in Fig. 4. The elastic potential energy of spring k_2 is derived as

$$\begin{aligned} U_{E,2} &= \frac{1}{2}k_2[c_3\mathbf{q}_3-(L-c_2)\mathbf{q}_2]^{\mathrm{T}}[c_3\mathbf{q}_3-(L-c_2)\mathbf{q}_2] \\ &= -k_2(L-c_2)c_3\mathbf{q}_2{}^{\mathrm{T}}\mathbf{q}_3 + \frac{1}{2}k_2(L-c_2)^2\mathbf{q}_2{}^{\mathrm{T}}\mathbf{q}_2 + \frac{1}{2}k_2c_3{}^2\mathbf{q}_3{}^{\mathrm{T}}\mathbf{q}_3 \end{aligned}. \tag{26}$$

The quadratic form of Eq. (26) yields the stiffness block matrix as

$$\mathbf{K}_{E,2} = \begin{bmatrix} \mathbf{0} & \mathbf{0} & \mathbf{0} \\ & \frac{1}{2}k_2(L-c_2)^2\mathbf{I} & -\frac{1}{2}k_2(L-c_2)c_3\mathbf{I} \\ \text{sym} & & \frac{1}{2}k_2c_3{}^2\mathbf{I} \end{bmatrix}. \tag{27}$$

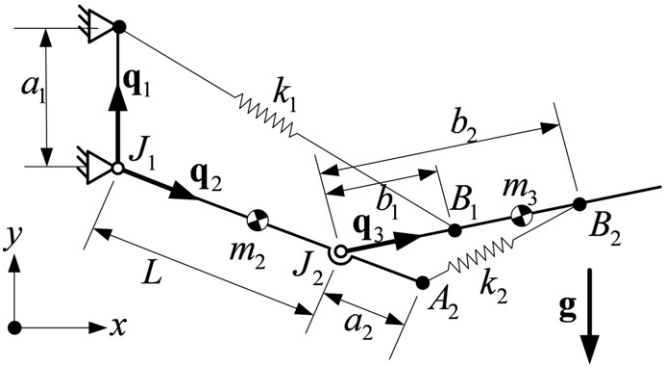

Fig. 5. The spring arrangement of the non-auxiliary-link design.

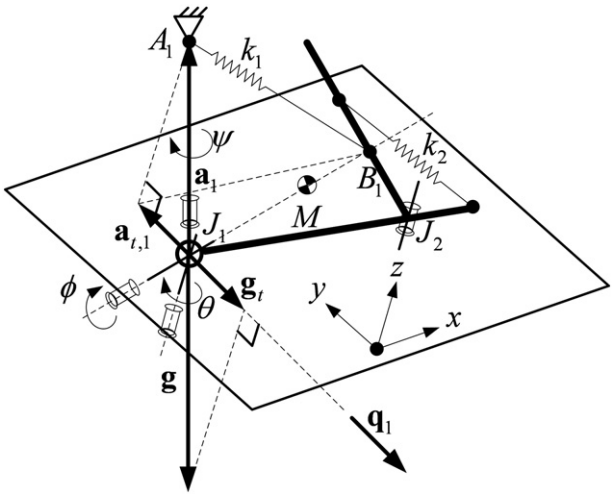

Fig. 6. The two-link model with 3 DOF on the shoulder joint and 1 DOF on the elbow.

Summing the stiffness block matrices Eqs. (16), (25) and (27) and letting the off-diagonal component matrices be zero matrices, the design equations of the system are derived as:

$$-k_1 a_1 + \mu g = 0 \tag{28}$$

$$k_1 c_2 - k_2 (L - c_2) = 0. \tag{29}$$

Since Eq. (29) is obtained by $\mathbf{K}_{23} = \mathbf{0}$, it suggests that a spring-to-spring balancing in the elbow flexion–extension $(\theta_3 - \theta_2)$ exists, and hence the two spring constants $k_1$and k_2 cannot be determined independently. Such pantograph balancing mechanisms are particularly useful while joint J_1 is either a revolute joint or a spherical joint. Since spring k_1 is attached to the mass center M, rotating the mechanism about line J_1M does not change the spring length A_1M, and consequently, neither the elastic potential energy nor the gravitational potential varies. This pantograph balancing mechanism was applied to a leg orthosis for gait training exercises [25]. Note that, since the lengths of the parallel links, namely c_3 and $(L - c_2)$, depend on the prescribed m_2 and m_3, the lengths of the parallel links are required to be adjusted to achieve an accurate balance according to the mass ratio of the upper arm and the forearm of an individual.

4. The planar 2-DOF spring balancing mechanisms without auxiliary links

A MAS with auxiliary links comprises closed-loop geometry in kinematics. It is robust in structure since the internal forces can be distributed by a number of links. However, arrangement of the auxiliary links in the system to prevent motion interference can be complicated. Besides, the closed-loop kinematic chain may reach to an uncertainty configuration when the links within the closed-loop are all collinear. In this section, a design without using auxiliary links is proposed.

Based on Eq. (16), as the non-zero $\mathbf{K}_{13}$ of the stiffness block matrix is to be eliminated, a spring can be directly fitted between links 1 and 3 as shown in Fig. 5. The elastic potential energy and its associated stiffness block matrix can be derived, respectively, as

$$\begin{aligned} U_{E,1} &= \frac{1}{2} k_1 (L\mathbf{q}_2 + b_1\mathbf{q}_3 - a_1\mathbf{q}_1)^{\mathrm{T}} (L\mathbf{q}_2 + b_1\mathbf{q}_3 - a_1\mathbf{q}_1) \\ &= -k_1 a_1 L \mathbf{q}_1{}^{\mathrm{T}}\mathbf{q}_2 - k_1 a_1 b_1 \mathbf{q}_1{}^{\mathrm{T}}\mathbf{q}_3 + k_1 L b_1 \mathbf{q}_2{}^{\mathrm{T}}\mathbf{q}_3 + \frac{1}{2} k_1 a_1{}^2 \mathbf{q}_1{}^{\mathrm{T}}\mathbf{q}_1 + \frac{1}{2} k_1 L^2 \mathbf{q}_2{}^{\mathrm{T}}\mathbf{q}_2 + \frac{1}{2} k_1 b_1{}^2 \mathbf{q}_3{}^{\mathrm{T}}\mathbf{q}_3 \end{aligned} \tag{30}$$

and

$$\mathcal{K}_{E,1} = \begin{bmatrix} \frac{1}{2} k_1 a_1{}^2 \mathbf{I} & -\frac{1}{2} k_1 a_1 L \mathbf{I} & -\frac{1}{2} k_1 a_1 b_1 \mathbf{I} \\ & \frac{1}{2} k_1 L^2 \mathbf{I} & \frac{1}{2} k_1 L b_1 \mathbf{I} \\ \text{sym} & & \frac{1}{2} k_1 b_1{}^2 \mathbf{I} \end{bmatrix}. \tag{31}$$

Since the installation of spring k_1 results in a non-zero $\mathbf{K}_{23}$, another spring is required to compensate the effect due to spring k_1. Thus, spring k_2 is fitted between links 2 and 3 with $\vec{J_2 A_2} = a_2\mathbf{q}_2$ and $\vec{J_2 B_2} = b_2\mathbf{q}_3$ as indicated in Fig. 5. The elastic potential energy of spring k_2 and its associated stiffness block matrix are expressed, respectively, as

$$U_{E,2} = \frac{1}{2} k_2 (b_2\mathbf{q}_3 - a_2\mathbf{q}_2)^{\mathrm{T}} (b_2\mathbf{q}_3 - a_2\mathbf{q}_2) = -k_2 a_2 b_2 \mathbf{q}_2{}^{\mathrm{T}}\mathbf{q}_3 + \frac{1}{2} k_2 a_2{}^2 \mathbf{q}_2{}^{\mathrm{T}}\mathbf{q}_2 + \frac{1}{2} k_2 b_2{}^2 \mathbf{q}_3{}^{\mathrm{T}}\mathbf{q}_3 \tag{32}$$

and

$$\mathcal{K}_{E,2} = \begin{bmatrix} \mathbf{0} & \mathbf{0} & \mathbf{0} \\ & \frac{1}{2}k_2{a_2}^2\mathbf{I} & -\frac{1}{2}k_2a_2b_2\mathbf{I} \\ \text{sym} & & \frac{1}{2}k_2{b_2}^2\mathbf{I} \end{bmatrix}. \tag{33}$$

By summing the stiffness block matrices of Eqs. (16), (31) and (33), and by having the off-diagonal component matrices $\mathbf{K}_{12}$, $\mathbf{K}_{13}$ and $\mathbf{K}_{23}$ to be zero matrices, design equations can be obtained as:

$$-k_1a_1L + \mu g c_2 = 0 \tag{34}$$

$$-k_1a_1b_1 + \mu g c_3 = 0 \tag{35}$$

$$k_1Lb_1 - k_2a_2b_2 = 0. \tag{36}$$

Springs k_1 and k_2 are referred to as a bi-articular spring and a mono-articular spring, respectively, according to the corresponding number of joints for which a spring is spanning over between the two attachment points. However, a bi-articular spring sometimes is required to transverse a potentially large workspace, and such a spring may be difficult to be obtained and manufactured. Thus, a trial-error process for determining the suitable spring constants and the reasonable spring attachment points is required. Without using parallel auxiliary links, this design requires generally less number of links and thus has a lighter weight. The adjustment of the upper arm length L is comparatively easier to achieve, while compared with a parallelogram linkage. Note that, the non-zero $\mathbf{K}_{23}$ induced by spring k_1 can also be compensated by another bi-articular spring k_2 fitted between links 1 and 3. However, such spring arrangement induces the coupled effects of the two springs. This indicates that either an imprecise spring constant k_1 or k_2 affects the gravity balancing on both the shoulder and the elbow motion.

5. Gravity balancing of the spatial 4-DOF spring assistive MAS

Design of a spatial 4-DOF MAS is proposed based on the spring arrangement of the planar 2-DOF spring balancing mechanism as shown in Fig. 5. By adding two extra rotational DOFs on the shoulder joint J_1 of the design, the MAS has a total of 4 DOFs. The gravity balancing of the spatial MAS is proved as effective as its planar case as follows.

As shown in Fig. 6, the upper arm and the forearm are lying in the xy-plane, and the spring attachments are the same as those in Fig. 5. The equivalent spherical joint J_1 can tilt the xy-plane with two independent rotations: Rotation ψ of the xy-plane about a vertical axis passing through point J_1; Rotation ϕ of the xy-plane about line J_1M. During the angular motion of ψ, the gravitational potential energy and the elastic potential energy are both constant since the altitudinal positions of the mass center M and all spring attachment points are not elevated or lowered during the motion.

During the angular motion of ϕ, the gravitational potential energy and the spring length of k_2 is kept constant. As shown in Fig. 6, if the attachment point B_1 of spring k_1 is on line J_1M, the spring length of k_1 can also be kept constant during the rotation ϕ.

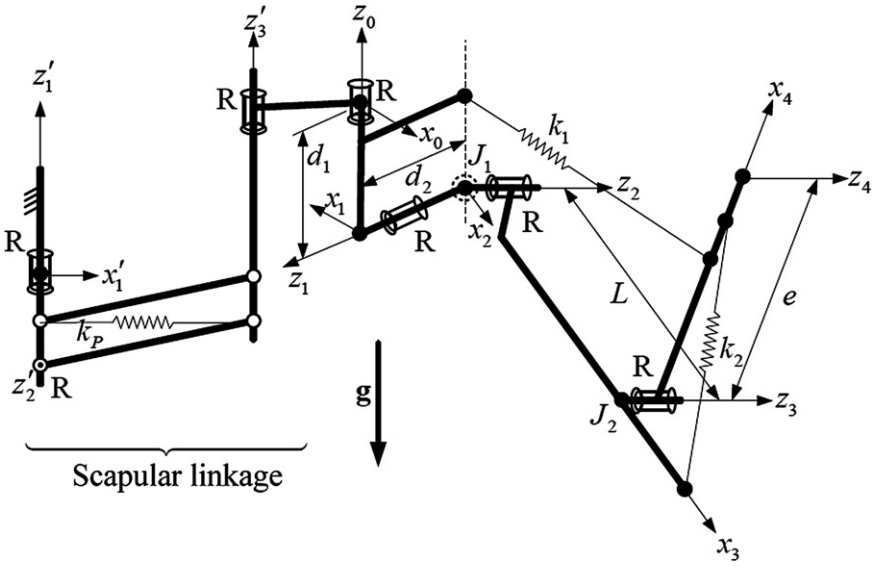

Fig. 7. Functional schematic of the spring assistive MAS.

Table 1
The Denavit–Hartenberg parameters of the arm linkage (d_i: the common normal between axes x_i and x_{i-1}; e_i: the common normal between axes z_i and z_{i-1}; α_i: the angle measured from axis z_{i-1} to axis z_i about axis x_i; θ_i: the joint angle from axis x_{i-1} to axis x_i about axis z_{i-1}).

Frame i	e_i	α_i	d_i	θ_i
1	0	$-\pi/2$	$-d_1$	θ_1
2	0	$3\pi/2$	$-d_2$	θ_2
3	L	0	0	θ_3
4	e	0	0	θ_4

As a result, the constant elastic potential energy of both springs k_1 and k_2 satisfies the static equilibrium. According to the design equations of the planar 2-DOF spring balancing mechanism, dividing Eq. (34) with Eq. (35) yields

$$\frac{L}{b_1}=\frac{c_2}{c_3}. \tag{37}$$

Vector $\vec{J_1B_1}=\mathbf{b}$ can be expressed as

$$\mathbf{b}=L\mathbf{q}_2+b_1\mathbf{q}_3=\rho c_2\mathbf{q}_2+\rho c_3\mathbf{q}_3 \tag{38}$$

where ρ is a constant ratio according to Eq. (37) as

$$\rho=\frac{L}{c_2}=\frac{b_1}{c_3}. \tag{39}$$

Judiciously from Eqs. (12) and (38),

$$\mathbf{b}=\rho\mathbf{c}. \tag{40}$$

Since $\mathbf{b}$ is parallel to the mass center position vector $\mathbf{c}$, point B_1 is on line J_1M, the design equations of Eqs. (34)–(36) are satisfied, and gravity balancing during motion ϕ can be achieved.

The third rotation θ of joint J_1 induces the planar motions of the upper arm and the forearm in the xy-plane. As defined in Fig. 5, vectors $\mathbf{q}_1$, $\mathbf{q}_2$ and $\mathbf{q}_3$ are in the xy-plane while vectors $\mathbf{g}$ and $\vec{J_1A_1}=\mathbf{a}_1$ remain vertical. Given the tilted xy-plane, projection of the gravitational acceleration vector $\mathbf{g}$ on the xy-plane is

$$\mathbf{g}_t=\mathbf{g}\cos\phi. \tag{41}$$

The gravitational acceleration vector of the projective model constrained to the xy-plane is $\mathbf{g}_t$. The projected position vector of the attachment point A_1 is

$$\mathbf{a}_{t,1}=\mathbf{a}_1\cos\phi. \tag{42}$$

The design equations of this projective model are identical to Eqs. (34)–(36) except for a multiplication factor of cos ϕ. Therefore, by additionally adding two rotational DOFs on the shoulder joint J_1, the static equilibrium state of the spatial 4-DOF MAS, constructed with all three rotations of the glenohumeral joint and one rotation of the elbow joint with two ideal zero-free-length springs, can be accomplished.

6. Adjusting gravity balancing of the spring assistive MAS

Since people have arms of different mass, calibration strategy is required to achieve a fine gravity balancing. In addition, some subjects may be able to withstand a portion of their limb weights and do not need a complete gravity balancing. Hence, the design parameters of the MAS to suit for any prescribed mass and dimension are derived and the adjustment strategy of gravity balancing of the MAS is also proposed.

Intuitively, the level of spring force can be managed by altering the spring stiffness or the positions of the spring attachment points. Since the WREX utilizes rubber bands as the spring elements, the desired spring constants can be adjusted simply by adding or removing a number of the rubber bands connected in parallel. However, for conventional metal springs, the adjustment

Table 2
Anthropometric parameters of the upper limb (data given in kg and m).

Upper arm	$m_2=2.18$	$s_2=0.210$	$L=0.332$
Forearm	$m_3=1.85$	$s_3=0.157$	

Table 3
Spring design parameters (data given in N/m and m).

Spring 1	$k_1 = 600$	$a_1 = 0.053$	$b_1 = 0.090$
Spring 2	$k_2 = 800$	$a_2 = 0.100$	$b_2 = 0.224$

is preferably achieved by moving the spring attachment points to desired positions. According to the design equations given in Eqs. (34)–(36), the design parameters of each spring attachment point can be derived as

$$a_1 = \left(\frac{gc_2}{k_1 L}\right)\mu \tag{43}$$

$$b_1 = \frac{c_3 L}{c_2} \tag{44}$$

$$a_2 b_2 = \frac{k_1 c_3 L^2}{k_2 c_2}. \tag{45}$$

According to Eq. (43), the distance between the attachment point A_1 and joint center J_1, or a_1, is the only parameter related to the system mass μ. By linearly displacing the attachment point A_1 to other positions, the gravity balancing of distinct levels can be adjusted precisely and quantitatively.

Adjusting gravity balancing of this proposed design is comparatively easier than that of the pantograph balancing mechanism because it requires changing only one spring attachment point. While the spring parameters of the two springs in the parallelogram balancing design are both dependent on μ as indicated in Eqs. (21) and (22), simultaneous change of the positions of the attachment points of the two springs is required.

7. The spring assistive MAS design

7.1. Schematic of the mechanical assembly

Human shoulder is a complex joint exhibiting a variety of movements through the glenohumeral joint and the shoulder girdle movement [26,27]. The shoulder motion is not exactly equivalent to a spherical joint motion. The rotation center of the glenohumeral joint changes its position more significantly during the high elevating motion of the upper arm [26,28]. In order to achieve a rigid attachment of an exoskeleton to the upper arm, Stienen et al. [29] proposed to mount the upper extremity exoskeleton device on a movable base so that an upper extremity exoskeleton possesses a total number of 6 DOFs at the shoulder joint to accommodate the three rotations and three translations of the glenohumeral joint.

Fig. 7 schematically shows the mechanical assembly of the MAS. The scapular linkage is to be mounted on a wheelchair, and it comprises a statically balanced parallelogram linkage to provide the moving mount for the shoulder joint J_1 and the spring attachment point A_1. Constituting of two vertical rotation axes z'_1 and z'_3 and one horizontal rotation axes z'_2 as indicated in Fig. 7,

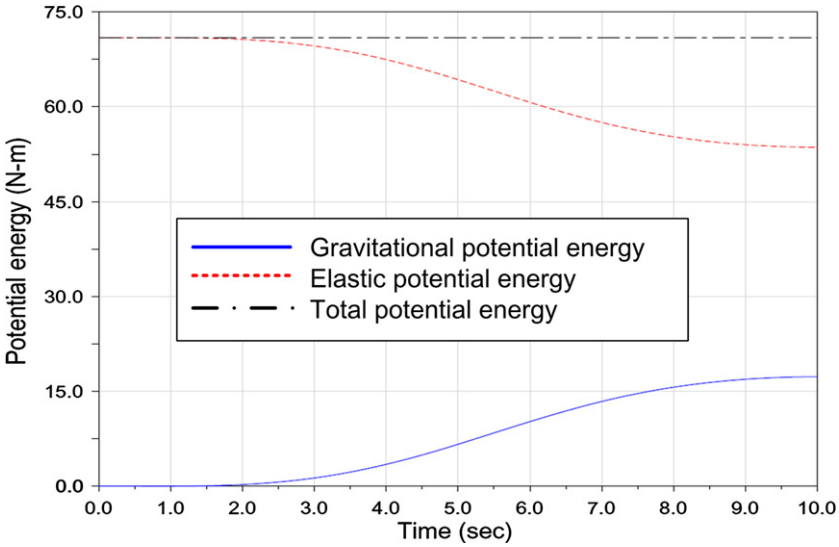

Fig. 8. The time history of the potential energies.

the scapular linkage provides a 3-DOF translation of the shoulder joint J_1. With such a linkage, the upper arm link has six DOFs with respect to the fixed frame. Hence, the upper arm link can be attached rigidly on the human upper arm without confining its motion even when the rotation axes of the shoulder joint J_1 is not perfectly aligned with the rotation axes of the glenohumeral joint. With the 3-DOF scapular linkage and the 4-DOF MAS linkage, a 7-DOF spatial spring assistive linkage is constructed. The MAS linkage has a total of four DOFs with rotation axes z_0, z_1, z_2 and z_3 in a serial connection, and the associated Denavit–Hartenberg parameters [30] are listed in Table 1.

Note that, since precise alignment between the human elbow joint axis and the joint axis of the device has been difficult [29], misalignment of the joints may cause uncomfortable or even painful feeling to the users due to the soft-tissue depression near the attachments [29,31]. A compensation strategy can be made through changing the position of the revolute joint axis z_3 to a proper location. Moreover, in practice, the perfect coincidence of the joint axes z_0, z_1 and z_2 to the human glenohumeral joint center J_1 is also difficult to achieve, and such arrangement of the joint axes may restrict the range of the horizontal rotation about z_1 or induce motion interference between the scapular link and the upper arm link of the MAS, especially when the upper arm is highly elevated. It is suggested that the joint axis z_0 can be shifted toward the back side of the human body, as indicated in Fig. 7, to avoid motion interference. This way, only joint axes z_1 and z_2 need to be aligned and alignment of these two joint axes can be achieved through the adjustment of the affixed position of the MAS to the upper arm.

7.2. Simulation

Simulation of the spring assistive MAS is based on a simplified 2-link model, jointed with J_1 and J_2, of the spring assistive MAS given in Fig. 7, where joint J_1 is a spherical joint mounted on ground. In the 2-link model based on the anthropometric and the statistic data [32–34], the dimensional and inertia parameters of the upper limb are listed in Table 2. Accordingly, design parameters of the attached springs can be obtained using Eqs. (43)–(45) and the results are listed in Table 3.

The simulations are implemented in software ADAMS. Angular displacements of the three rotations on the shoulder and the elbow flexion–extension are prescribed to achieve a combing hair motion, a common activity of daily living (ADL) [35], from a rested position where the upper arm and the forearm are, respectively, in vertical and horizontal orientations as their initial configuration. Since the dynamic effect and the muscular compliance force are assumed negligible in the slow operation of the MAS, the static-mode simulation is utilized. The interference effects were also neglected. The time history of the gravitational potential energy and the elastic potential energy are plotted in Fig. 8, where the total potential energy of the system is constant during the grooming motion and all static torques sustaining the weight of the upper limb are zero. The maximum spring forces induced by springs k_1 and k_2 are 237 N and 233 N, respectively, which fit in a reasonable range. The maximum forces supported by the bearings of the elbow joint and the shoulder joint are 198 N and 197 N, respectively.

8. Conclusion

Spring balancing mechanism encompasses a variety of methods to arrange the configuration of the spring connections. Each arrangement has its own advantages and disadvantages over a particular application. This paper investigates the underlying theories of some existing spring balancing mechanisms. Comparisons of the parallelogram design, the pantograph design and the non-auxiliary-link design are also discussed. A novel non-auxiliary-link design of a spring assistive MAS with a simpler structure and easiness for the adjustments is proposed. In the non-auxiliary-link design, its physical interaction among the spring forces and the gravitational forces is similar to the pantograph design. The primary spring is connected from the base to the forearm link accomplishing the major weight balance of the mechanism, and the secondary spring has been used for the spring-to-spring balance in the elbow motion. Since the design parameters of the two springs have coupled effects, the spring-to-spring balancing results in an additional design equation, and thus the free design parameters in the proposed MAS design are less than those in the parallelogram design by one. However, this design is advantageous in adapting to different levels of gravity balancing. The gravity balancing of the proposed MAS is verified through a static-mode simulation of ADAMS that was carried out over a sample motion of the MAS.

References

[1] L.W. Pedretti, M.B. Early, Occupational Therapy: Practice Skills for Physical Dysfunction, 5th ed. Mobsby, St. Louis, MO, 2001.
[2] S. Landsberger, P. Leung, V. Vargas, J. Shaperman, J. Baumgarten, L.Y. Yasuda, E. Sumi, D. McNeal, R. Waters, Mobile arm supports: history, application, and work in progress, Topics in Spinal Cord Injury Rehabilitation 11 (2) (2005) 74–94.
[3] R.L. Bennett, The evolution of the Georgia Warm Springs Foundation Feeder, Artificial Limb 10 (1) (1966) 5–9.
[4] JAECO Orthopedic [home page on the Internet]. Available from: http://www.jaeco-orthopedic.com.
[5] T. Rahman, W. Sample, S. Jayakumar, M.M. King, J.Y. Wee, R. Seliktar, M. Alexander, M. Scavina, A. Clark, Passive exoskeletons for assisting limb movement, Journal of Rehabilitation Research and Development 43 (5) (2006) 583–590.
[6] T. Rahman, W. Sample, R. Seliktar, M.T. Scavina, A.L. Clark, K. Moran, M.A. Alexander, Design and testing of a functional arm orthosis in patients with neuromuscular diseases, IEEE Transactions on Neural Systems and Rehabilitation Engineering 15 (2) (2007) 244–251.
[7] J.L. Herder, N. Vrijlandt, T. Antonides, M. Cloosterman, P. Mastenbroek, Principle and design of a mobile arm support for people with muscular weakness, Journal of Rehabilitation Research and Development 43 (5) (2006) 591–604.
[8] A. Stienen, E. Hekman, G. Prange, M. Jannink, F. van der Helm, H. van der Kooij, Freebal: design of a dedicated weight-support system for upper-extremity rehabilitation, ASME Journal of Medical Devices 3 (2009) 041009.
[9] A. Russo, R. Sinatra, Fengfeng Xi, Static balancing of parallel robots, Mechanism and Machine Theory 40 (2) (2005) 191–202.

[10] V.H. Arakelian, M.R. Smith, Shaking force and shaking moment balancing of mechanisms: a historical review with new examples, ASME Journal of Mechanical Design 127 (2) (2005) 334–339.
[11] K. Koser, A cam mechanism for gravity-balancing, Mechanics Research Communications 36 (4) (2009) 523–530.
[12] I. Simionescu, L. Ciupitu, The static balancing of the industrial robot arms part II: continuous balancing, Mechanism and Machine Theory 35 (9) (2000) 1299–1311.
[13] J.L. Herder, Design of spring force compensation systems, Mechanism and Machine Theory 33 (1–2) (1998) 151–161.
[14] P.-Y. Lin, W.-B. Shieh, D.-Z. Chen, A stiffness matrix approach for the design of statically balanced planar articulated manipulators, Mechanism and Machine Theory 45 (2010) 1877–1891.
[15] P.-Y. Lin, W.-B. Shieh, D.-Z. Chen, Design of a gravity-balanced general spatial serial-type manipulator, ASME Journal of Mechanisms and Robotics 2 (2009) 031003.
[16] D.A. Streit, E. Shin, Equilibrators for planar linkages, ASME Journal of Mechanical Design 115 (3) (1993) 604–611.
[17] R.H. Nathan, A constant force generation mechanism, ASME Journal of Mechanisms, Transmissions, and Automation in Design 107 (12) (1985) 508–512.
[18] S.K. Agrawal, A. Fattah, Gravity-balancing of spatial robotic manipulator, Mechanism and Machine Theory 39 (12) (2004) 1331–1344.
[19] J.L. Herder, G.M. Tuijthof, Design, actuation and control of an anthropomorphic robot arm, Mechanism and Machine Theory 35 (2000) 945–962.
[20] T. Rahman, R. Ramanathan, R. Seliktar, W. Harwin, A simple technique to passively gravity-balance articulated mechanisms, ASME Journal of Mechanical Design 117 (4) (1995) 655–658.
[21] W.D. Van Dorsser, R. Barents, B.M. Wisse, M. Schenk, J.L. Herder, Energy-free adjustment of gravity equilibrators by adjusting the spring stiffness, Proceedings of the Institution of Mechanical Engineers, Part C: Journal of Mechanical Engineering Science 222 (9) (2008) 1839–1846.
[22] K.N. An, A.O. Browne, S. Korinek, S. Tanaka, B.F. Morrey, Three-dimensional kinematics of glenohumeral elevation, Journal of Orthopaedic Research 9 (1) (1991) 143–149.
[23] N. Yang, M. Zhang, C. Huang, D. Jin, Synergic analysis of upper limb target-reaching movements, Journal of Biomechanics 35 (2002) 739–746.
[24] D.P. Romilly, C. Anglin, R.G. Gosine, C. Herdhler, S.U. Raschke, A functional task analysis and motion simulation for the development of a powered upper-limb exoskeleton, IEEE Transactions on Rehabilitation Engineering 2 (3) (1994) 119–129.
[25] S.K. Agrawal, A. Fattah, Theory and design of an orthotic device for full or partial gravity-balancing of a human leg during motion, IEEE Transactions on Neural Systems And Rehabilitation Engineering 12 (2) (2004) 157–165.
[26] T. Nef, R. Riener, Shoulder actuation mechanisms for arm rehabilitation exoskeletons, in: Proceedings of the 2nd Biennial IEEE/RAS-EMBS International Conference on Biomedical Robotics and Biomechatronics, Scottsdale, AZ, USA, October 19–22 2008.
[27] V.M. Zatsiorsky, Kinematics of Human Motion, Human Kinetics, Champaign, IL, 1997.
[28] T.B. Moeslund, C.B. Madsen, E. Granum, Modelling the 3D pose of a human arm and the shoulder complex utilising only two parameters, Integrated Computer-Aided Engineering 12 (2005) 159–175.
[29] A. Stienen, E. Hekman, F. van der Helm, H. van der Kooij, Self-aligning exoskeleton axes through decoupling of joint rotations and translations, IEEE Transactions on Robotics 25 (3) (2009) 628–633.
[30] J. Denavit, R.S. Hartenberg, A kinematic notation for lower pair mechanisms based on matrices, ASME Journal of Applied Mechanics 77 (1955) 215–221.
[31] I. Russell, Depression and soft tissue pain, Journal of Musculoskeletal Pain 11 (1) (2003) 1–3.
[32] NASA Reference Publication 1024, Anthropometric Source Book: Volume I: Anthropometry for Designers, NASA, 1978.
[33] R.F. Chandler, C.E. Clauser, J.P. McConville, H.M. Reynolds, J.W. Young, Investigation of Inertia Properties of the Human Body, Final Report, Apr. 1, 1972–Dec. 1974. AMRL-TR-74-137 Aerospace Medical Research Laboratories, Wright-Patterson Air Force Base, Dayton, Ohio, 1975.
[34] C.E. Clauser, J.T. McConville, J.W. Young, Weight, Volume and Center of Mass of Segmens of the Human Body. AMRL-TR-69-70 Aerospace Medical Research Laboratories, Wright-Patterson Air Force Base, Dayton, Ohio, 1969. (NASA CR-11262).
[35] D.J. Magermans, E. Chadwick, H. Veeger, F. van der Helm, Requirements for upper extremity motions during activities of daily living, Clinical biomechanics 20 (6) (2005) 591–599.